

# Monte Carlo study of the pairing interaction in the two-leg Hubbard ladder

N. Bulut, T. Dahm and D.J. Scalapino

*Department of Physics, University of California*

*Santa Barbara, CA 93106-9530*

## Abstract

Monte Carlo calculations of the irreducible particle-particle interaction on a two-leg Hubbard ladder doped near half-filling are reported. As the temperature is lowered, this interaction develops structure in momentum space similar to the magnetic susceptibility  $\chi(\mathbf{q})$  and reflects the development of strong short-range antiferromagnetic correlations. Using this interaction, the eigenfunction of the leading singlet pair eigenvalue is found to have  $d_{x^2-y^2}$  like symmetry. The single-particle spectral weight is also shown to peak near  $(\pi, 0)$  and  $(0, \pi)$  when the ratio of the inter- to intra-chain hopping  $t_{\perp}/t \simeq 1.5$ , leading to an increased tendency for pairing.

Numerical calculations, renormalization-group bosonization studies as well as strong-coupling treatments find that half-filled  $t$ - $J$  or Hubbard two-leg ladders have a spin gapped ground state with short range antiferromagnetic correlations [1–3]. Furthermore, these various techniques all find that when holes are doped into the ladder,  $d_{x^2-y^2}$ -like pairing correlations develop. This being the case, one would like to understand the nature of the effective interaction that gives rise to the  $d_{x^2-y^2}$  pairing correlations for this system. Here, in order to address this question, we present Monte Carlo results for the irreducible particle-particle interaction  $\Gamma_I$ . In addition, we use  $\Gamma_I$  and the single-particle Green's function obtained from the Monte Carlo calculations to solve the Bethe-Salpeter equation in the singlet pairing channel. We find that the eigenfunction with the leading eigenvalue has  $d_{x^2-y^2}$ -like symmetry.

The Hubbard model Hamiltonian for a two-leg ladder has the form

$$H = -t \sum_{i,\lambda,s} (c_{i\lambda s}^\dagger c_{i+1\lambda s} + \text{h.c.}) - t_\perp \sum_{i,s} (c_{i1s}^\dagger c_{i2s} + \text{h.c.}) + U \sum_{i\lambda} n_{i\lambda\uparrow} n_{i\lambda\downarrow}. \quad (1)$$

Here  $t$  is the intra-chain one electron hopping,  $t_\perp$  the inter-chain hopping and  $U$  the on-site Coulomb interaction. The operators  $c_{i\lambda s}^\dagger$  and  $c_{i\lambda s}$  create and destroy electrons of spin  $s$  on site  $i$  of the  $\lambda^{\text{th}}$  leg, respectively, and  $n_{i\lambda s} = c_{i\lambda s}^\dagger c_{i\lambda s}$  is the occupation number for spin  $s$  on site  $i$  of the  $\lambda^{\text{th}}$  leg.

Using Monte Carlo techniques, we have calculated the finite temperature two-particle Green's function

$$G_2(x_4, x_3, x_2, x_1) = -\langle T c_\uparrow(x_4) c_\downarrow(x_3) c_\downarrow^\dagger(x_2) c_\uparrow^\dagger(x_1) \rangle. \quad (2)$$

Here  $c_s^\dagger(x_i)$  with  $x_i = (\mathbf{x}_i, \tau_i)$  creates an electron of spin  $s$  at site  $\mathbf{x}_i$  and imaginary time  $\tau_i$  and  $T$  is the usual  $\tau$ -ordering operator. Then, as previously discussed [4], one can take the Fourier transform of both the space and imaginary time variables and obtain  $G_2(p', k', k, p)$  with  $p' = (\mathbf{p}', i\omega_n)$ , etc. This two particle Green's function can be expressed in terms of the exact single-particle propagator  $G_s(\mathbf{p}, i\omega_n)$  and the reducible particle-particle vertex  $\Gamma(p', k', k, p)$

$$\begin{aligned}
G_2(p', k', k, p) = & -\delta_{p,p'} \delta_{k,k'} G_{\downarrow}(k) G_{\uparrow}(p) \\
& + \frac{T}{N} \delta_{p'+k', p+k} G_{\uparrow}(p') G_{\downarrow}(k') \Gamma(p', k', k, p) G_{\downarrow}(k) G_{\uparrow}(p).
\end{aligned} \tag{3}$$

Then from the Monte Carlo data for  $G$  and  $G_2$ , one can determine  $\Gamma(p', k', k, p)$ . Finally, because the effective pairing interaction corresponds to the irreducible particle-particle interaction  $\Gamma_I$  in the zero energy and momentum center of mass channel, we have inverted the fully dressed  $t$ -matrix equation to find  $\Gamma_I$  in terms of  $\Gamma$  and  $G$ . Setting  $k = -p$  and  $k' = -p'$ , the fully dressed  $t$ -matrix equation becomes

$$\Gamma(p'|p) = \Gamma_I(p'|p) - \frac{T}{N} \sum_k \Gamma(p'|k) G_{\downarrow}(-k) G_{\uparrow}(k) \Gamma_I(k|p), \tag{4}$$

which is solved to find  $\Gamma_I(p'|p)$ . The effective pairing interaction in the singlet channel is

$$V(p' - p) = \frac{1}{2} (\Gamma_I(p'|p) + \Gamma_I(-p'|p)). \tag{5}$$

We have carried out this calculation at different temperatures for various values of the hopping anisotropy  $t_{\perp}/t$ , interaction strength  $U/t$  and filling  $\langle n \rangle = \langle n_{i\uparrow} + n_{i\downarrow} \rangle$ . Here, we will show results for  $t_{\perp}/t = 1.5$ ,  $U/t = 4$  and  $\langle n \rangle = 0.875$ . We have chosen this set of parameters, because the numerical density matrix renormalization group (DMRG) calculations find that for  $U/t = 4$  and  $\langle n \rangle = 0.875$ , the  $d_{x^2-y^2}$  pairing correlations are strongest when  $t_{\perp}/t \simeq 1.5$  [5]. In addition, for these parameters we have good control of the maximum entropy analytic continuation of the Monte Carlo data, which is necessary to obtain the single-particle spectral weight  $A(\mathbf{p}, \omega)$ .

In Fig. 1 we plot the effective pairing interaction  $V$  versus  $q_x = p'_x - p_x$  for  $q_y = p'_y - p_y = \pi$ . Here we have set  $\omega_n = \omega_{n'} = \pi T$  corresponding to  $\omega_m = 0$  energy transfer. The three curves correspond to temperatures  $T = 1.0t$ ,  $0.5t$  and  $0.25t$ . One can see that as the temperature decreases, the effective pairing interaction becomes increasingly positive at large momentum transfer  $\mathbf{q} \rightarrow (\pi, \pi)$ . As shown in Figure 2, the magnetic susceptibility

$$\chi(\mathbf{q}) = \frac{1}{N} \int_0^{\beta} d\tau \sum_{\ell} e^{i\mathbf{q}\cdot\ell} \langle m_{i+\ell}^-(\tau) m_i^+(0) \rangle \tag{6}$$

also develops structure at large momentum transfers over this same temperature region. Thus it is clear that the effective pairing interaction is associated with the development of short-range antiferromagnetic correlations.

It is also of interest to study the Bethe-Salpeter equation for the singlet particle-particle channel

$$\lambda_\alpha \phi_\alpha(\mathbf{p}, i\omega_n) = -\frac{T}{N} \sum_{\mathbf{p}', i\omega_{n'}} \Gamma_I(\mathbf{p}, i\omega_n | \mathbf{p}', i\omega_{n'}) |G(\mathbf{p}', i\omega_{n'})|^2 \phi_\alpha(\mathbf{p}', i\omega_{n'}). \quad (7)$$

Fig. 3 shows the eigenfunction  $\phi(\mathbf{p}, i\omega_n)$  of the leading eigenvalue versus  $\mathbf{p}$  for  $\omega_n = \pi T$ . We observe that  $\phi(\mathbf{p}, i\pi T)$  has  $d_{x^2-y^2}$ -like momentum structure in the sense that it has opposite signs and is largest near  $(\pi, 0)$  on the bonding band and near  $(0, \pi)$  on the antibonding band. This is associated with the structure of the irreducible interaction  $\Gamma_I$  and the single-particle spectral weight  $A(\mathbf{p}, \omega)$  which we will study below [6].

The temperature dependence of the leading eigenvalue  $\lambda_1$  is plotted in Fig. 4(a). As previously discussed, when the temperature is lowered, short-range antiferromagnetic correlations develop and the effective pairing interaction increases at large momentum transfer. This leads to an increase in  $\lambda_1$  as shown in Fig. 4(a). We believe that  $\lambda_1$  will approach unity at low temperatures where power-law  $d_{x^2-y^2}$ -like pairing correlations have been shown to exist using density matrix renormalization group techniques [2]. In Fig. 4(b), we show the dependence of the leading eigenvalue  $\lambda_1$  on the hopping anisotropy  $t_\perp/t$ . According to the DMRG calculations [5], for  $U/t = 4$  and  $\langle n \rangle = 0.875$  the pairing correlations in the ground state are strongest when  $t_\perp/t \simeq 1.5$ . In Fig. 4(b), we do not observe a strong dependence of  $\lambda_1$  on  $t_\perp/t$  because of the thermal smearing effects at  $T = 0.25t$ .

In addition to the irreducible interaction vertex  $\Gamma_I$ , the single-particle Green's function  $G(\mathbf{p}, i\omega_n)$  is also important in determining the structure of the leading eigenfunction of the Bethe-Salpeter equation. Using a numerical maximum entropy procedure [7], we have calculated the single-particle spectral weight

$$A(\mathbf{p}, \omega) = -\frac{1}{\pi} \text{Im} G(\mathbf{p}, \omega). \quad (8)$$

This is plotted in Fig. 5 for  $t_{\perp}/t = 1.5$  as a function of  $\omega$  for different  $\mathbf{p}$ . Here, the solid curves are for the bonding band ( $p_y = 0$ ) and the dotted curves are for the antibonding band ( $p_y = \pi$ ). We see that for this value of  $t_{\perp}/t$ , the bonding band has spectral weight near the Fermi level for  $\mathbf{p} \sim (\pi, 0)$ , and the antibonding band has spectral weight near the Fermi level for  $\mathbf{p} \sim (0, \pi)$ . Hence, these Fermi points can be connected by scatterings involving  $\mathbf{q} = (\pi, \pi)$  momentum transfer. Since  $\Gamma_{IS}$  is large and repulsive for  $\mathbf{q} \sim (\pi, \pi)$ , the leading eigenfunction  $\phi$  of the Bethe-Salpeter equation has opposite signs for  $\mathbf{p}$  near  $\mathbf{p} = (\pi, 0)$  and  $(0, \pi)$ , as seen in Fig. 3.

These calculations provide further insight into the structure of the effective pairing interaction and the single-particle spectral weight which lead to the pairing correlations in the two-leg Hubbard ladder. Specifically, the momentum structure of the effective interaction  $V(\mathbf{q})$  clearly reflects the existence of short-range antiferromagnetic correlations as the cause of the increasing positive strength of  $V(\mathbf{q})$  at large momentum transfer. Secondly, the enhanced spectral weight in the bonding band near  $(\pi, 0)$  and the antibonding band near  $(0, \pi)$  are reminiscent of a similar effect observed in the two-dimensional Hubbard model near half-filling [8,9] and in the ARPES of the cuprates [10]. This enhanced low lying spectral weight associated with the renormalized quasiparticles is such that pair scattering processes with momentum transfers near  $(\pi, \pi)$  have increased phase space. These two features appear to play an important role in the development of pairing on the two-leg ladder, just as they do for the two-dimensional Hubbard model.

## ACKNOWLEDGMENTS

The authors gratefully acknowledge support from the National Science Foundation under Grant No. DMR95-27304 and PHY94-07194, and from the Deutsche Forschungsgemeinschaft. The numerical computations reported in this paper were performed at the San Diego Supercomputer Center.

## REFERENCES

- [1] T.M. Rice, S. Gopalan and M. Sigrist, *Europhys. Lett.* **23**, 445 (1993); H. Tsunetsugu, M. Troyer and T.M. Rice, *Phys. Rev. B* **49**, 16078 (1994).
- [2] R.M. Noack, S.R. White and D.J. Scalapino, *Phys. Rev. Lett.* **73**, 882 (1994); *Physica C* **270**, 281 (1996).
- [3] L. Balents and M.P.A. Fisher, *Phys. Rev. B* **53**, 12133 (1996).
- [4] N. Bulut, D.J. Scalapino and S.R. White, *Phys. Rev. B* **47**, 2742 (1993).
- [5] R.M. Noack, N. Bulut, D.J. Scalapino and M.G. Zacher, preprint.
- [6] We note that as  $t_{\perp}/t$  is varied, the momentum structure of the single-particle spectral weight and the irreducible interaction changes. Consequently, the momentum structure of the leading eigenfunction  $\phi$  changes. A discussion of how  $\phi$  is affected by  $t_{\perp}/t$  and further results on the doping dependence will be given in a longer article. Here, we concentrate on a set of parameters for which the DMRG calculations find enhanced pairing correlations.
- [7] S.R. White, *Phys. Rev. B* **44**, 4670 (1991).
- [8] N. Bulut, D.J. Scalapino and S.R. White, *Phys. Rev. B* **50**, 7215 (1994).
- [9] R. Preuss, W. Hanke and W. von der Linden, *Phys. Rev. Lett.* **75**, 1344 (1995).
- [10] For a review, see Z.-X. Shen and D.S. Dessau, *Physics Reports* **253**, 1 (1995).

## FIGURES

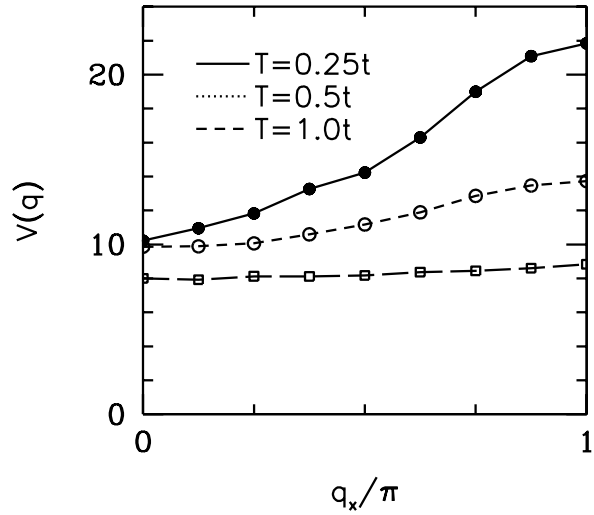


FIG. 1. Momentum dependence of the effective interaction  $V(\mathbf{q})$  for  $U = 4t$ ,  $\langle n \rangle = 0.875$  and  $t_{\perp} = 1.5t$ . Here  $V(\mathbf{q})$  is measured in units of  $t$ .

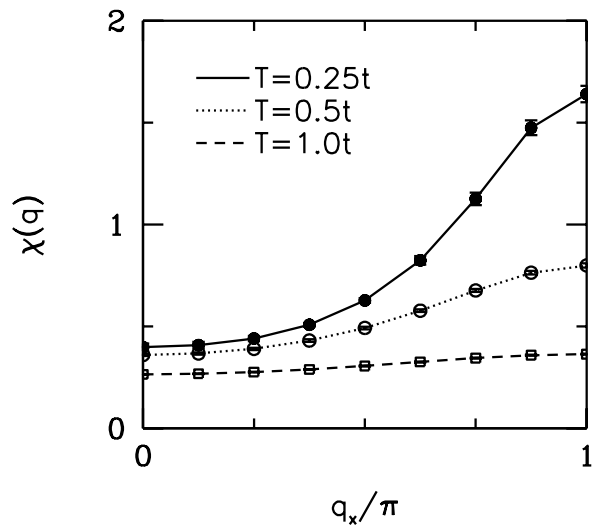


FIG. 2. Momentum dependence of the magnetic susceptibility  $\chi(\mathbf{q})$  for  $U = 4t$ ,  $\langle n \rangle = 0.875$  and  $t_{\perp} = 1.5t$ .

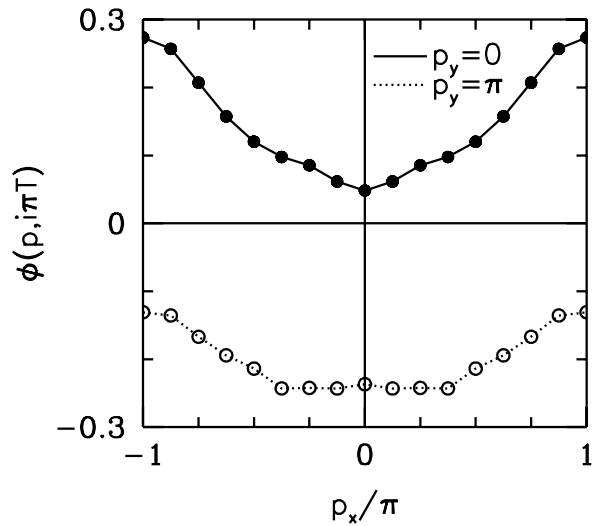


FIG. 3. Momentum dependence of the  $d_{x^2-y^2}$  eigenfunction  $\phi(\mathbf{p}, i\pi T)$ . These results are for  $T = 0.25t$ ,  $U = 4t$ ,  $\langle n \rangle = 0.875$  and  $t_\perp = 1.5t$ .

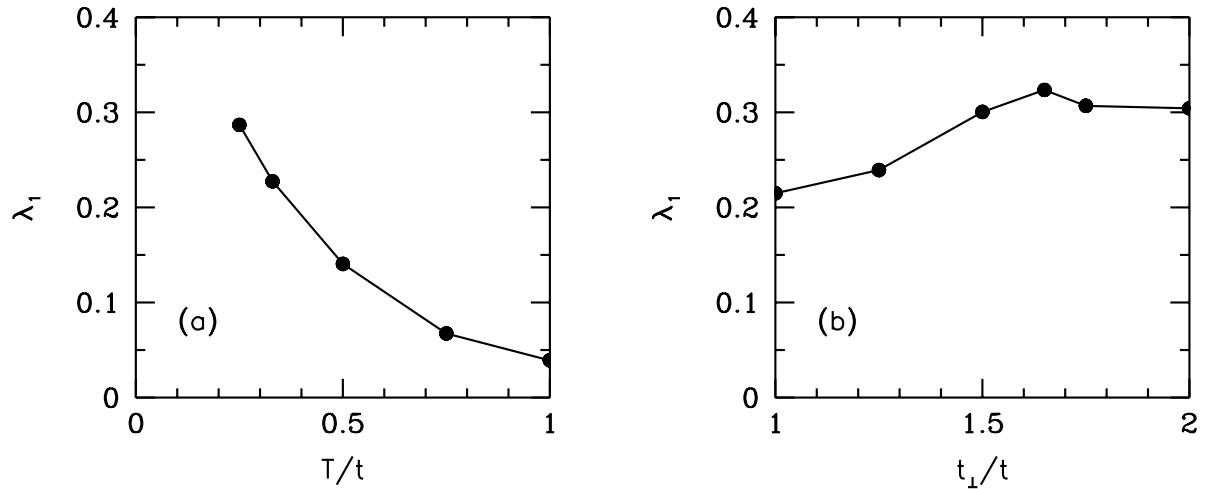


FIG. 4. (a) Temperature dependence of the leading eigenvalue  $\lambda_1$  for  $t_\perp = 1.5t$ . (b)  $\lambda_1$  vs  $t_\perp/t$  for  $T = 0.25t$ . These results are for  $\langle n \rangle = 0.875$  and  $U = 4t$ .

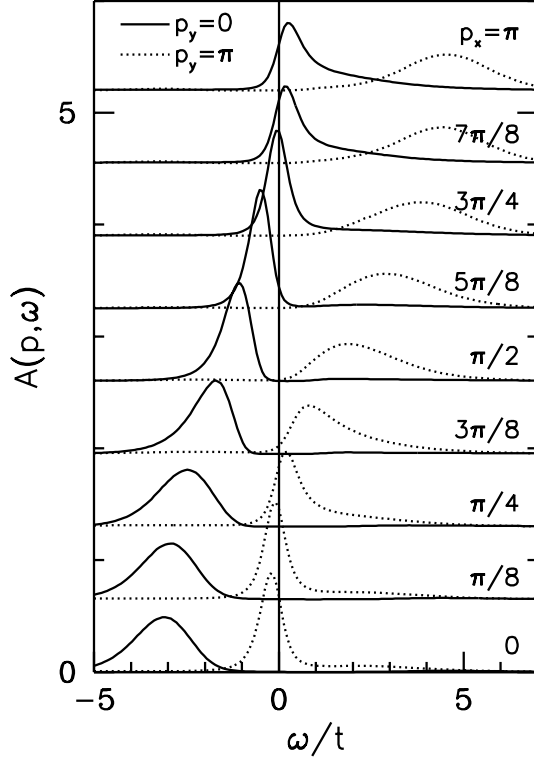


FIG. 5. Single-particle spectral weight  $A(\mathbf{p}, \omega)$  versus  $\omega$  for  $t_{\perp}/t = 1.5$ ,  $T = 0.25t$  and  $\langle n \rangle = 0.875$ . The solid curves denote the results for the bonding band ( $p_y = 0$ ) and the dotted curves denote the results for the antibonding band ( $p_y = \pi$ ).